CrossMark

ORIGINAL PAPER

Strength/Brittleness Classification of Igneous Intact Rocks Based on Basic Physical and Dynamic Properties

Saeed Aligholi[1] · Gholam Reza Lashkaripour[1] · Mohammad Ghafoori[1]

Abstract This paper sheds further light on the fundamental relationships between simple methods, rock strength, and brittleness of igneous rocks. In particular, the relationship between mechanical (point load strength index $I_{s(50)}$ and brittleness value S_{20}), basic physical (dry density and porosity), and dynamic properties (P-wave velocity and Schmidt rebound values) for a wide range of Iranian igneous rocks is investigated. First, 30 statistical models (including simple and multiple linear regression analyses) were built to identify the relationships between mechanical properties and simple methods. The results imply that rocks with different Schmidt hardness (SH) rebound values have different physicomechanical properties or relations. Second, using these results, it was proved that dry density, P-wave velocity, and SH rebound value provide a fine complement to mechanical properties classification of rock materials. Further, a detailed investigation was conducted on the relationships between mechanical and simple tests, which are established with limited ranges of P-wave velocity and dry density. The results show that strength values decrease with the SH rebound value. In addition, there is a systematic trend between dry density, P-wave velocity, rebound hardness, and brittleness value of the studied rocks, and rocks with medium hardness have a higher brittleness value. Finally, a strength classification chart and a brittleness classification table are presented, providing reliable and low-cost methods for the classification of igneous rocks.

List of symbols

ρ	Dry density
ϕ	Porosity
V_p	P-wave velocity
R_N	Schmidt rebound number
S_{20}	Brittleness value
$I_{s(50)}$	Point load strength index
M	P-wave modulus
σ_{zz}	Axial stress
ε_{zz}	Axial strain
H	Hardness
ε	Strain
M_{VRH}	Voigt–Reuss–Hill average
M_V	Voigt upper bound effective elastic modulus
M_R	Reuss lower bound effective elastic modulus
f	Volume fraction
M_{Rk}	Rock effective P-wave modulus
σ_{max}	Maximum stress

1 Introduction

Estimation/classification of mechanical properties of rocks plays a key role in the design in any rock engineering project. Strength and brittleness characteristics are two important geotechnical parameters used in rock engineering projects such as tunneling and underground openings, dam foundations, drilling, and slope stability analysis.

Intact rock material strength is classified based on uniaxial compressive strength (UCS) or point load index test results (Bieniawski 1989; Ghosh and Srivastava 1991). The point load test is an attractive alternative to the UCS

✉ Gholam Reza Lashkaripour
  lashkaripour@um.ac.ir

[1] Department of Geology, Faculty of Science, Ferdowsi University of Mashhad, Mashhad, Iran

because it can provide similar data at a lower cost (Gurocak et al. 2012). Moreover, the point load strength index correlates closely with uniaxial tensile and compressive strengths and can be used to predict other strength parameters (Reichmuth 1968; Broch and Franklin 1972; ISRM 1985; Hawkins 1998; Lashkaripour 2002; Palchik and Hatzor 2004; Heidari et al. 2012; Kohno and Maeda 2012; Li and Wong 2013).

So far, no internationally accepted norm has been proposed for measurement and determination of the rock brittleness. There are some definition of brittleness for different purposes (Ramsey 1967; Obert and Duvall 1967; Andreev 1995), and various methods for determination of rock brittleness (Protodyakonov 1963; Hunka and Das 1974; Lawn and Marshall 1979; Quinn and Quinn 1997; Blindheim and Bruland 1998; Yagiz 2002, 2009a; Copur et al. 2003) can be found in the literature (Altindag 2010; Dursun and Gokay 2016). Brittleness characteristics of rocks substantiality affect their mechanical performance, drillability, cuttability, and machine performance. Some research studies were performed to investigate the relationship between brittleness, cuttability, and penetrability of different rocks (Singh 1986; Kahraman et al. 2003; Hajiabdolmajid and Kaiser 2003; Gong and Zhao 2007; Altindag 2010; Yarali and Kahraman 2011; Dursun and Gokay 2016). Brittleness test was developed in Sweden by von Matern and Hjelmer (1943). The original test was aimed to determine the strength properties of aggregates, but several modified versions of the test have later been developed for various purposes (Dahl et al. 2012). In this study, the version S_{20} of brittleness test, developed for the determination of rock drillability, is employed for brittleness classification of Iranian igneous rocks.

Careful sample preparation for precise determination of rock strength parameters as well as brittleness value in the laboratory can be tedious, costly, and time-consuming and involve destructive tests. However, relations between the simple methods (density, porosity, P-wave velocity, and hardness tests) and the brittleness have not been investigated in detail yet probably due to the lack of a standardized universal measurement method exactly defining or measuring the rock brittleness. In contrast, there are various studies in the literature proposing empirical correlations between strength properties and simple methods of different rocks (Deere and Miller 1966; Inoue and Ohomi 1981; Shorey et al. 1984; Katz et al. 2000; Kahraman 2001; Kilic and Teymen 2008; Sharma and Singh 2008; Yagiz 2009b; Khandelwal and Ranjith 2010; Gupta and Sharma 2012). Although a variety of empirical equations have been reported from these studies, it is inconclusive yet to develop empirical equations for different rocks. Moreover, the empirical equations often

have a very low accuracy of estimation and suffer from insufficient generalization ability (Liu et al. 2014). There are two main explanations for this behavior: (1) the differences in regional tectonic setups, the genesis of the rocks and environmental conditions such as temperature and hydrothermal solution that cause different degrees of alteration and weathering and (2) using only a single factor during the modeling process. Most problems in mining and geology involve complex and interacting forces, which are impossible to isolate and study separately (Davis 1973). Mechanical properties of rocks might be affected by multiple factors such as hardness, toughness, density, porosity, fractures and discontinuities, weathering and alterations, and mineral composition and texture features. Hence, for a reliable and robust classification/prediction of rock strength parameters, a reasonable combination of given parameters is required. Recently, multivariate regression models and artificial intelligence-based models such as artificial neural network, fuzzy logic, and genetic algorithm are employed by some researchers for rock strength prediction from simple methods (Karakus and Tutmez 2006; Gurocak et al. 2012; Monjezi et al. 2012; Rabbani et al. 2012; Rezaei et al. 2012; Yagiz et al. 2012; Beiki et al. 2013; Minaeian and Ahangari 2013). The results provided by such works are more satisfactory compared to those of simple regression analysis. However, computational intelligence techniques also have some limitations such as the local minimum problem, inappropriately high number of parameters, and inefficient learning in practice. Furthermore, the results of these methods are difficult to be explained physically since they are incapable of revealing the mechanisms between the input parameters and the targets (Liu et al. 2014). As a conclusion, to understand relations between various physicomechanical properties and classify rocks from different regions, an extensive study is required to be conducted.

In this study, detailed investigations of the effects of dry density, porosity, P-wave velocity, and Schmidt rebound number to rock strength and brittleness are carried out. By now, there is limited knowledge of the effect of physical and dynamic characteristics on the brittleness of rocks. The aim of this study is to analyze the fundamental relationships between simple parameters and strength and brittleness of igneous rocks and present the methods applied for fast classification of such rocks. By these models, the brittleness and strength are classified using the parameters obtained from simple methods. These models can be used for initial cost analysis and project planning as a decision-making index. The major difference between this study and the previous works is that the strength and brittleness of rocks are predicted using classification methods presented in this work.

2 Experimental Material

A total of 44 various types of igneous rocks were sampled in 15 different locations in Iran based on a preliminary desk study as well as the macroscopic structure and visible features of the selected rocks. Then, considering sampling location and microscopic analysis, the samples were separated into 28 rock groups for further investigations. The sampling locations of the rocks are shown in Fig. 1. A wide range of igneous rocks (plutonic and extrusive) are examined in this study. The majority of the plutonic rocks were felsic (granitoid) and some intermediate to mafic rocks (gabbro and diorite), while the extrusive rocks mostly involve andesite and basalt. Modal analysis of the studied rocks is presented in Table 1. According to Anon (1995), all samples were unweathered or slightly weathered. Blocks were carefully checked to ensure they are homogeneous and free from visible weaknesses.

3 Physicomechanical Tests

Each block sample was drilled or cut to obtain cylindrical cores or blocky specimens to inspect the physical, dynamic, and mechanical properties. Also, thin sections were prepared from each rock sample for petrographic analysis. Various standard test procedures were carried out to determine properties of the studied rocks. The basic physical properties of the rock samples including density and porosity were measured according to ISRM (1981). The P-wave velocity was determined using a portable ultrasonic nondestructive digital indicating tester (PUNDIT) according to ISRM (2007). Rebound hardness values of the

Fig. 1 Location map of the rock samples

rock samples were determined according to the procedure suggested by the ISRM (Aydin 2009) using an N-type Proceq Schmidt hammer on blocky samples. To do so, the hammer was held vertically downward and at right angles to the horizontal rock faces. Brittleness value tests were conducted following the procedure suggested by (Dahl 2003). Point load strength test was performed on blocky or core samples (axial test) according to ISRM (1985). The results are shown in Table 2.

4 Statistical Analyses

This study aims to analyze the relationships between simple parameters and strength and brittleness of igneous rocks and present the methods applied for fast classification of such rocks. In order to describe the relationships between point load strength index $I_{s(50)}$ as well as brittleness value S_{20} and simple tests such as dry density (ρ), porosity (ϕ), P-wave velocity (V_p) and Schmidt rebound number (R_N) of the tested rocks, mainly two statistical models, namely simple linear regression model and multiple regression models, were applied with a 95 % confidence level.

4.1 Simple Linear Regression Models

Concerning the relations between the dependent and independent variables, first of all, simple linear regression analyses were carried out by considering linear functions (models 1–4). The results of the regression analyses are given in Table 3. In table and Figs. 2 and 3, meaningful correlations were found between P-wave velocity and dry density with both strength and brittleness of the rocks. As shown in Figs. 2 and 3, in each case, the best-fitted relation was represented by the linear regression curves. In addition, as shown in Figs. 2d and 3d, no correlation can be established between rebound values and both point load strength indices and brittleness values. However, it can be clearly seen that if SH rebound values are classified, then correlations will provide more satisfactory results. Based on this observation, the obtained data were sorted and (according to rebound values) classified into seven rock hardness classes (Table 4). The relations between point load strength index $I_{s(50)}$ and brittleness value S_{20} with simple tests for each hardness class are illustrated in Figs. 4 and 5, respectively. As shown in Figs. 2d, 3d, 4 and 5, for each case, the best-fitted relation between dependent and independent variables for all hardness classes was obtained by the linear regression curves (Table 5). Then, once again, simple regression analysis between mechanical and simple method tests was carried out for each hardness class. The results of correlations between the measured and predicted

Table 1 Modal analysis and rock names of the studied rocks

Rock code	Qtz (%)	Pl (%)	Afs (%)	Bt (%)	Ms (%)	Am (%)	Chl (%)	Cpx (%)	Opx (%)	Ol (%)	Grt (%)	OM (%)	Ep (%)	Gl (%)	AM < 1 %	Rock name[a]
R1	28	35	20	17	–	–	–	–	–	–	–	–	–	–	Zrn	Micro-monzogranite
R2	38	24	28	3	7	–	–	–	–	–	–	–	–	–	–	Monzogranite
R3	31	21	34	4	9	–	1	–	–	–	–	–	–	–	–	Monzogranite
R4	–	41	–	–	–	5	–	8	5	–	2	2	1	36	–	Hyalo-basaltic andesite
R5	32	34	27	4	–	2	–	–	–	–	–	1	–	–	–	Monzogranite
R6	–	47	–	–	–	4	–	19	5	9	–	13	3	–	–	Basalt
R7(a)	38	24	27	9	–	1	1	–	–	–	–	–	–	–	Zrn	Monzogranite
R7(b)	39	19	33	5	–	2	2	–	–	–	–	–	–	–	Zrn	Monzogranite
R7(c)	35	23	34	7	–	–	1	–	–	–	–	–	–	–	–	Monzogranite
R8(a)	39	22	30	7	–	1	1	–	–	–	–	–	–	–	Zrn	Monzogranite
R8(b)	31	13	47	6	–	1	2	–	–	–	–	–	–	–	Zrn	Syenogranite
R8(c)	43	12	40	3	–	1	1	–	–	–	–	–	–	–	–	Syenogranite
R8(d)	35	26	33	4	–	1	1	–	–	–	–	–	–	–	Zrn	Monzogranite
R9(a)	46	14	36	2	–	1	1	–	–	–	–	–	–	–	Zrn	Syenogranite
R9(b)	39	16	40	2	–	1	2	–	–	–	–	–	–	–	Zrn	Syenogranite
R9(c)	39	13	44	2	–	–	2	–	–	–	–	–	–	–	Zrn	Syenogranite
R10	26	17	48	6	–	–	1	–	–	–	–	–	2	–	–	Syenogranite
R11(a)	13	35	7	8	–	3	–	–	–	–	–	3	–	31	–	Hyalo-dacite
R11(b)	13	34	8	10	–	2	–	–	–	–	–	3	–	30	–	Hyalo-dacite
R11(c)	11	32	7	9	–	3	–	–	–	–	–	3	–	35	–	Hyalo-dacite
R12	29	38	22	4	–	3	2	–	–	–	1	1	–	–	–	Monzogranite
R13	14	46	16	–	–	12	9	–	–	–	–	3	–	–	Zrn	Quartz monzodiorite
R14	12	59	3	–	–	7	9	4	–	–	–	6	–	–	–	Andesite
R15(a)	1	63	1	4	–	22	4	–	–	–	1	4	–	–	Spn	Diorite
R15(b)	1	64	1	2	–	24	2	–	–	–	1	5	–	–	Spn	Diorite
R16	4	63	6	–	–	14	8	–	–	–	–	5	–	–	–	Andesite
R17(a)	33	29	31	4	–	–	3	–	–	–	–	–	–	–	–	Monzogranite
R17(b)	25	28	38	5	–	–	4	–	–	–	–	–	–	–	–	Monzogranite
R18	–	48	–	4	–	3	–	16	6	–	9	6	8	–	–	Gabbro
R19	–	36	–	5	–	7	–	18	11	14	–	2	7	–	–	Gabbro
R20	–	57	2	4	–	6	–	–	11	8	1	5	6	–	Zrn	Diorite
R21(a)	–	57	2	4	–	5	–	13	3	8	–	4	4	–	–	Diorite
R21(b)	–	59	4	4	–	2	–	13	3	6	2	4	3	–	–	Diorite
R22(a)	14	31	39	1	–	12	–	–	–	–	–	3	–	–	–	Quartz monzonite
R22(b)	12	35	43	1	–	6	–	–	–	–	–	3	–	–	–	Quartz monzonite
R23(a)	8	39	43	1	–	7	–	–	–	–	–	2	–	–	–	Quartz monzonite
R23(b)	6	41	45	1	–	5	–	–	–	–	–	2	–	–	–	Quartz monzonite
R24	12	24	56	2	–	4	–	–	–	–	–	2	–	–	–	Quartz syenite
R25	3	69	7	4	–	14	–	–	–	–	–	3	–	–	–	Andesite
R26(a)	23	45	19	5	–	4	2	–	–	–	–	2	–	–	Spn	Granodiorite
R26(b)	31	36	19	6	–	5	–	–	–	–	–	3	–	–	Spn	Granodiorite
R26(c)	26	41	20	6	–	4	1	–	–	–	–	2	–	–	Spn	Granodiorite

Table 1 continued

Rock code	Qtz (%)	Pl (%)	Afs (%)	Bt (%)	Ms (%)	Am (%)	Chl (%)	Cpx (%)	Opx (%)	Ol (%)	Grt (%)	OM (%)	Ep (%)	Gl (%)	AM < 1 %	Rock name[a]
R27	29	45	9	7	–	6	2	–	–	–	1	1	–	–	Spn	Granodiorite
R28	–	59	–	8	–	5	–	12	4	–	–	2	6	4	–	Micro-gabbro

Qtz—quartz, Pl—plagioclase, Afs—alkali feldspar, Bt—biotite, Ms—muscovite, Am—amphibole, Chl—chlorite, Cpx—clinopyroxene, Opx—orthopyroxene, Ol—olivine, Grt—garnet, OM—opaque minerals, Ep—epidote, Gl—glass, AM—accessory minerals, Zrn—zircon, Spn—sphene

[a] According to optical microscopy studies (Streckeisen 1976)

values, based on hardness classification and simple regression analysis (models 5–8), are given in Table 6.

As shown in Tables 3 and 6, only model 4 fails to reject the null hypothesis at the default $\alpha = 0.05$ significance level and the other relationships are statistically significant. To control the performance of the equations obtained from proposed models, the root-mean-square error (RMSE) was calculated for each model from the following formula:

$$RMSE = \sqrt{\frac{1}{N} \sum_{i=1}^{N} \left(y_i - y_i' \right)} \tag{2.1}$$

where y and y' are, respectively, the measured and predicted values and N is the number of samples. If the R squared is 1 and RMSE is 0, the model proposed would be excellent. Also, the Pearson's correlation coefficient (R) is calculated using the following equation:

$$R_{xy} = \frac{\text{cov}(x, y)}{s_x s_y} \tag{2.2}$$

where to find the correlation between the variables, covariance is divided by the standard deviation values for each simple regression model.

4.2 Multiple Linear Regression Analysis

Mechanical properties of rocks such as strength and brittleness are affected by multiple factors such as hardness, toughness, density, porosity, fractures and discontinuities, weathering and alterations, mineral composition, and texture features. Rock brittleness is a combination of rock properties rather than a single parameter (Dursun and Gokay 2016). The brittleness value S_{20} is influenced not only by the mineralogical composition of the rock, grain size, and grain binding, but also, to a great extent, by the degree of weathering/alteration, micro-fracturing, and foliation (Dahl et al. 2012). Naturally, all factors cannot be included in a simple test. But, if more variables are incorporated in mechanical properties prediction of rock materials, more reliable results would be achieved.

In this study, 22 different multiple linear regression models were applied to correlate the dependent and independent variables. Eleven different compositions (Table 7) of the simple tests were employed to understand which model (no. 9–19) is suitable for strength and brittleness classification of igneous rocks. Table 8 presents the results of multiple regression models (no. 20–30) between the measured and predicted values after hardness classification. As shown in Tables 6 and 8, it is obvious that in both simple and multiple linear regression models, correlations mostly have a significant improvement in comparison with those shown in Tables 3 and 7. From the results, it might be concluded that there are meaningful relationships between hardness and mechanical properties of rocks. In other words, rocks with different hardness values have different physicomechanical properties.

The influence of each parameter can be found by comparing the statistical parameters of models together. As shown in Table 8, among the predictive models with two independent variables (models 20–25), model 21 is the best one for prediction of both point load strength index and brittleness value. Between predictive models with three independent variables (models 26–29), models 26 and 28 are the best ones for prediction of both $I_{s(50)}$ and S_{20}. In Table 8, compared to the best models with three dependent variables, model 30 which applies all simple test parameters as independent variables does not show any further improvement. On the basis of this statistical research, it can be concluded that integration of simple tests and SH rebound value classification has shown good performance and accuracy to mechanical properties prediction of igneous rocks.

In this study, to check the validation of the statistical models, the measured mechanical properties were plotted versus the predicted mechanical properties from most beneficial models (Fig. 7). As shown in Fig. 7a–f, the points are distributed nearly uniformly around the diagonal line that proved the validity of proposed models. Moreover, the boxes showing the classification ranges of the mechanical properties are given in these figures, such boxes could show performance of these models for the task of rock classification. It is notable that, based on $I_{s(50)}$ classification ranges given by Bieniawski (1984), the point load strength results of the studied igneous rocks grouped

Table 2 Characteristics of the studied rocks

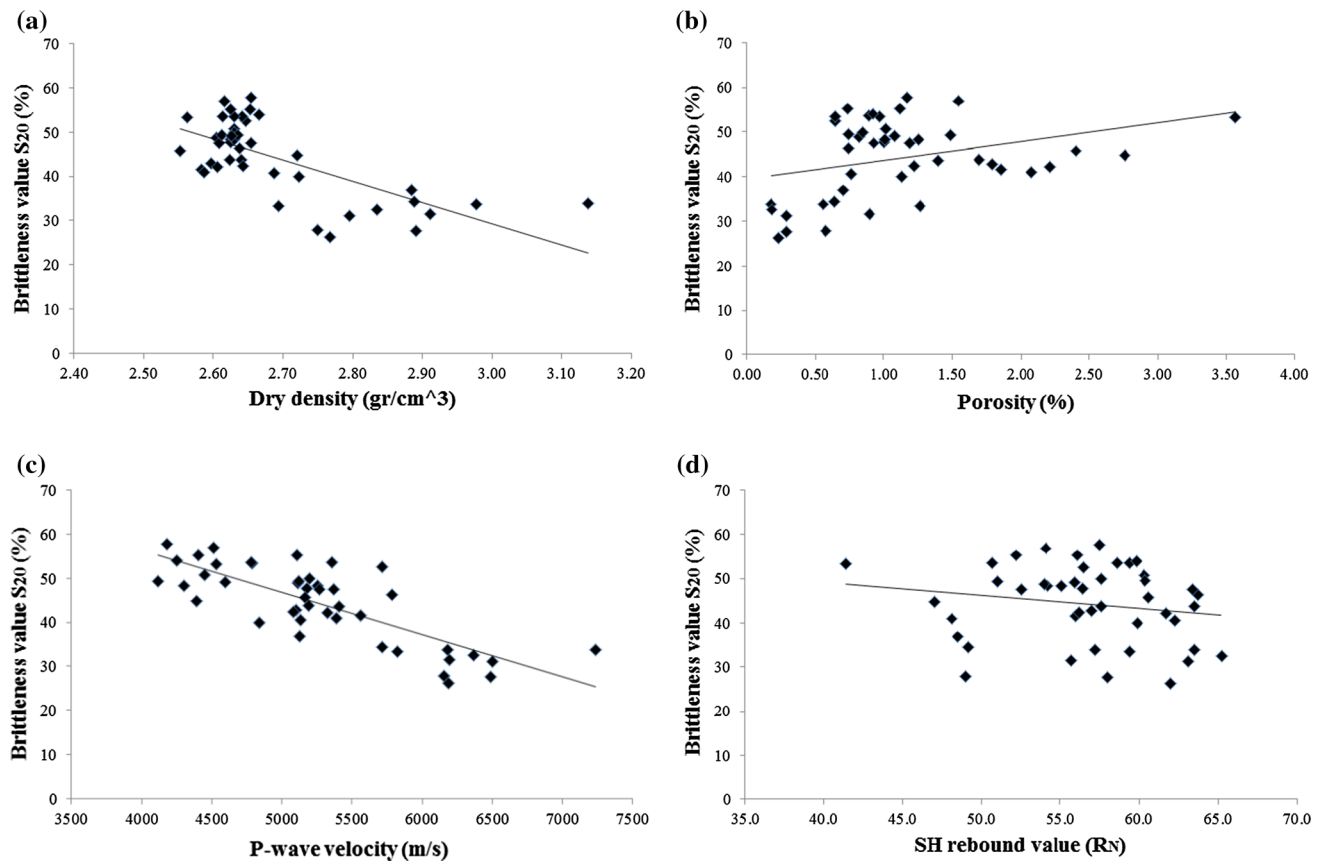| Rock code	Dry density (g/cm^3)	Porosity (%)	P-wave velocity (m/s)	SH rebound value (R_N)	Brittleness value S_{20} (%)	Point load strength index $I_{s(50)}$ (MPa)
R1	2.72	1.13	4841	59.9	40.02	6.14
R2	2.63	1.01	4451	60.3	50.8	6.72
R3	2.62	1.25	4301	54.2	48.31	5.63
R4	2.65	0.65	5715	56.5	52.55	9.78
R5	2.64	1.40	5406	63.5	43.69	7.77
R6	2.91	0.89	6193	55.7	31.55	14.64
R7$_{(a)}$	2.64	0.65	5360	59.4	53.6	8.41
R7$_{(b)}$	2.62	1.00	5180	56.4	47.7	7.52
R7$_{(c)}$	2.61	0.97	4787	58.6	53.5	7.23
R8$_{(a)}$	2.63	0.89	4783	50.70	53.6	7.74
R8$_{(b)}$	2.63	1.01	5252	55.10	48.4	7.23
R8$_{(c)}$	2.62	0.73	5106	56.10	55.2	8.05
R8$_{(d)}$	2.60	0.82	5116	54.00	48.9	7.57
R9$_{(a)}$	2.61	0.93	5269	52.50	47.5	9.54
R9$_{(b)}$	2.63	0.85	5198	57.60	50.0	7.81
R9$_{(c)}$	2.61	0.74	5120	60.40	49.5	8.71
R10	2.69	0.76	5136	62.3	40.66	5.49
R11$_{(a)}$	2.58	1.86	5563	56.00	41.6	9.89
R11$_{(b)}$	2.59	2.08	5388	48.10	41.0	11.71
R11$_{(c)}$	2.60	1.79	5103	57.00	42.9	9.12
R12	2.64	1.49	4115	51	49.3	7.78
R13	2.72	2.76	4394	47	44.82	8.36
R14	2.75	0.57	6156	49	27.95	12.29
R15$_{(a)}$	2.89	0.64	5716	49.20	34.4	11.22
R15$_{(b)}$	2.89	0.71	5128	48.50	36.9	12.64
R16	2.69	1.26	5825	59.4	33.4	8.69
R17$_{(a)}$	2.63	1.08	4598	55.90	49.2	7.20
R17$_{(b)}$	2.62	1.55	4513	54.10	56.9	6.62
R18	2.98	0.55	6182	57.2	33.81	11.41
R19	3.14	0.18	7239	63.5	33.85	12.29
R20	2.83	0.18	6365	65.2	32.53	11.08
R21$_{(a)}$	2.77	0.23	6185	62.0	26.33	11.57
R21$_{(b)}$	2.79	0.29	6500	63.1	31.18	10.16
R22$_{(a)}$	2.61	2.21	5328	61.70	42.2	6.59
R22$_{(b)}$	2.55	2.40	5165	60.60	45.7	7.41
R23$_{(a)}$	2.64	1.22	5082	56.2	42.3	8.52
R23$_{(b)}$	2.62	1.70	5189	57.6	43.8	7.86
R24	2.56	3.57	4531	41.4	53.31	5.59
R25	2.64	0.74	5783	63.7	46.3	10.49
R26$_{(a)}$	2.67	0.92	4248	59.8	54.0	7.44
R26$_{(b)}$	2.65	1.12	4406	52.2	55.2	7.91
R26$_{(c)}$	2.65	1.17	4178	57.5	57.7	6.46
R27	2.65	1.19	5367	63.4	47.56	6.07
R28	2.89	0.29	6491	58	27.65	10.68

Table 3 Statistic parameters of simple linear regression between mechanical and simple test parameters

Model no.	Dependent variable	Independent variable	Predictive model	RMSE	R	R^2	Adj. R^2	p value
1	Point load strength index (MPa)	Dry density (g/cm³)	$I_{s(50)} = 11.916\,\rho - 23.337$	1.63	0.67	0.45	0.44	0.000
2		Porosity (%)	$I_{s(50)} = -1.336\,\phi + 10.207$	2.00	−0.42	0.18	0.16	0.004
3		P-wave velocity (m/s)	$I_{s(50)} = 0.0022\,V_p - 3.096$	1.51	0.73	0.53	0.52	0.000
4		SH rebound value (R_N)	$I_{s(50)} = -0.023\,R_N + 10.007$	2.20	−0.06	0.00	−0.02	0.721
1	Brittleness value S_{20} (%)	Dry density (g/cm³)	$S_{20} = -47.92\,\rho + 173.11$	6.39	−0.68	0.47	0.45	0.000
2		Porosity (%)	$S_{20} = 4.143\,\phi + 36.60$	8.25	0.33	0.11	0.09	0.028
3		P-wave velocity (m/s)	$S_{20} = -0.0095\,V_p + 94.564$	5.44	−0.78	0.61	0.60	0.000
4		SH rebound value (R_N)	$S_{20} = -0.290\,R_N + 60.699$	8.61	−0.18	0.03	0.01	0.252
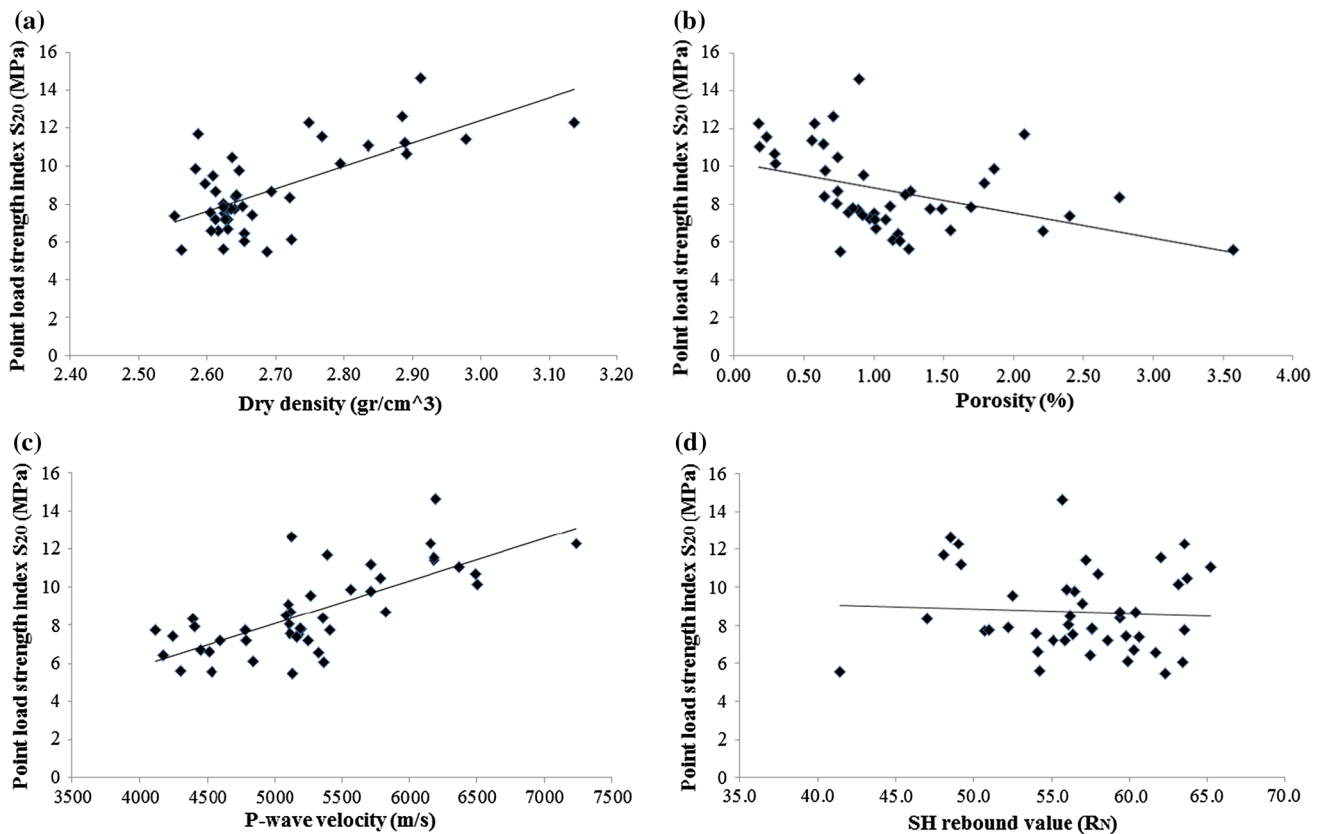
Fig. 2 Point load strength index $I_{s(50)}$ versus simple methods: **a** dry density, **b** porosity, **c** P-wave velocity, and **d** SH rebound value (R_N)

only into the "high" and "very high" strength classes. In this study, based on the statistical distribution of the point load strength index $I_{s(50)}$ values and the background of the authors, four categories of strength are proposed (Fig. 6a). These new categories are more accurate for classification of hard (stronger) rocks. Furthermore, it is more appropriate for validation of results from this study. According to the proposed strength classification for hard rocks, the

studied rocks are assigned to one of the following four classes: class MH—moderately high strength, for point load strength index between 5.00 and 7.49 MPa, class H—high strength (7.50–9.99 MPa); class VH—very high strength (10.00–11.99 MPa), and class EH—extremely high strength (greater than 12.00 MPa). Classification of brittleness value S_{20} given in Fig. 6b, which is based on the study of Dahl et al. (2012), is according to the statistical
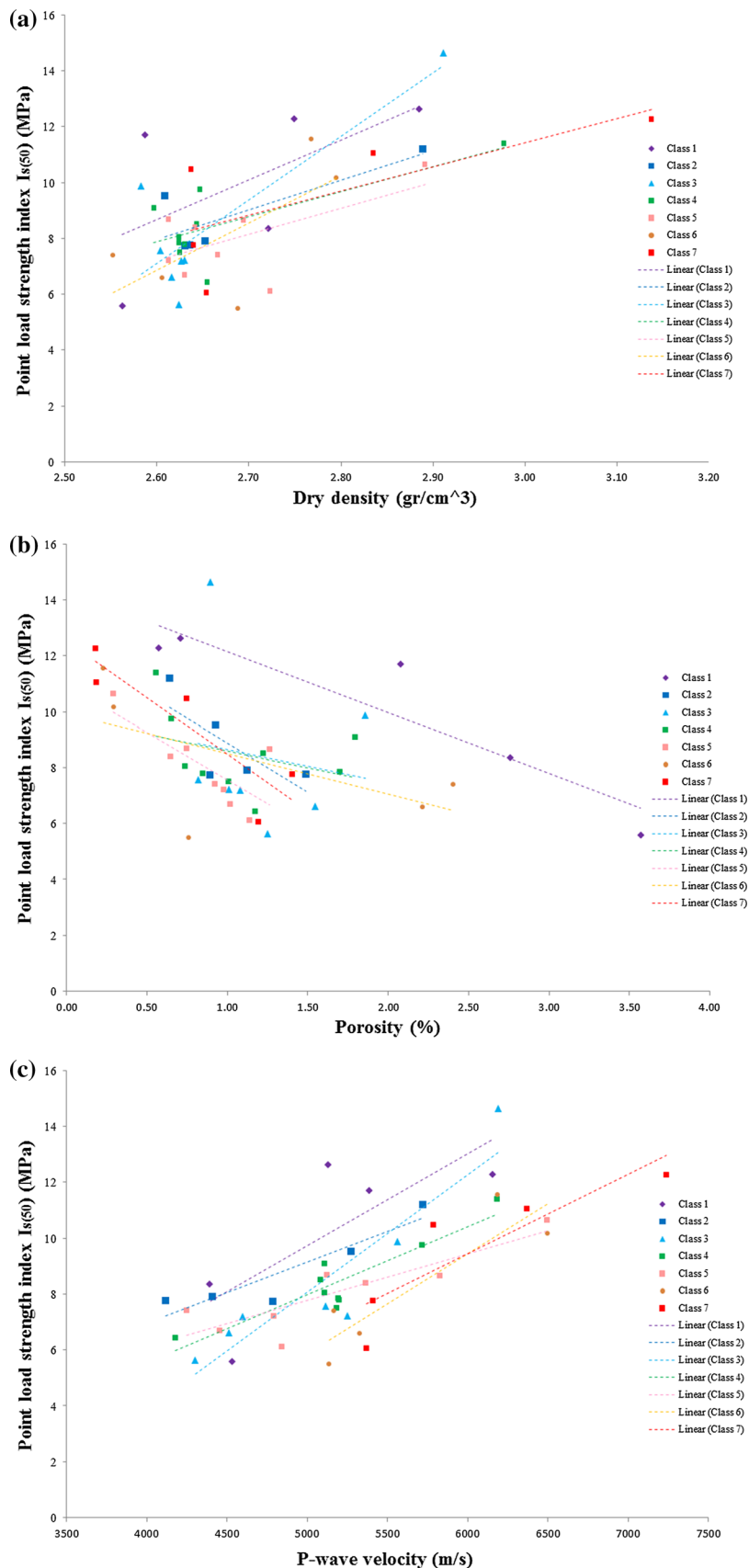
Fig. 3 Brittleness value S_{20} versus simple methods: **a** dry density, **b** porosity, **c** P-wave velocity, and **d** SH rebound value (R_N)

Table 4 Rock hardness classes

Rock code	SH rebound value (R_N)	Hardness class	Rock code	SH rebound value (R_N)	Hardness class	Rock code	SH rebound value (R_N)	Hardness class
R24	41.4	1	R8$_{(c)}$	56.10	4	R22$_{(b)}$	60.60	6
R13	47		R23$_{(a)}$	56.2		R22$_{(a)}$	61.70	
R11$_{(b)}$	48.10		R7$_{(b)}$	56.4		R21$_{(a)}$	62.0	
R15$_{(b)}$	48.50		R4	56.5		R10	62.3	
R14	49		R11$_{(c)}$	57.00		R21$_{(b)}$	63.1	
R15$_{(a)}$	49.20	2	R18	57.2		R27	63.4	7
R8$_{(a)}$	50.70		R26$_{(c)}$	57.5		R5	63.5	
R12	51		R9$_{(b)}$	57.60		R19	63.5	
R26$_{(b)}$	52.2		R23$_{(b)}$	57.6		R25	63.7	
R9$_{(a)}$	52.50		R28	58	5	R20	65.2	
R8$_{(d)}$	54.00	3	R7$_{(c)}$	58.6				
R17$_{(b)}$	54.10		R7$_{(a)}$	59.4				
R3	54.2		R16	59.4				
R8$_{(b)}$	55.10		R26$_{(a)}$	59.8				
R6	55.7		R1	59.9				
R17$_{(a)}$	55.90		R2	60.3				
R11$_{(a)}$	56.00		R9$_{(c)}$	60.40				

Fig. 4 Point load strength index $I_{s(50)}$ versus different parameters for each hardness class: **a** dry density, **b** porosity, and **c** P-wave velocity

Fig. 5 Brittleness value S_{20} versus different parameters for each hardness class: **a** dry density, **b** porosity, and **c** P-wave velocity
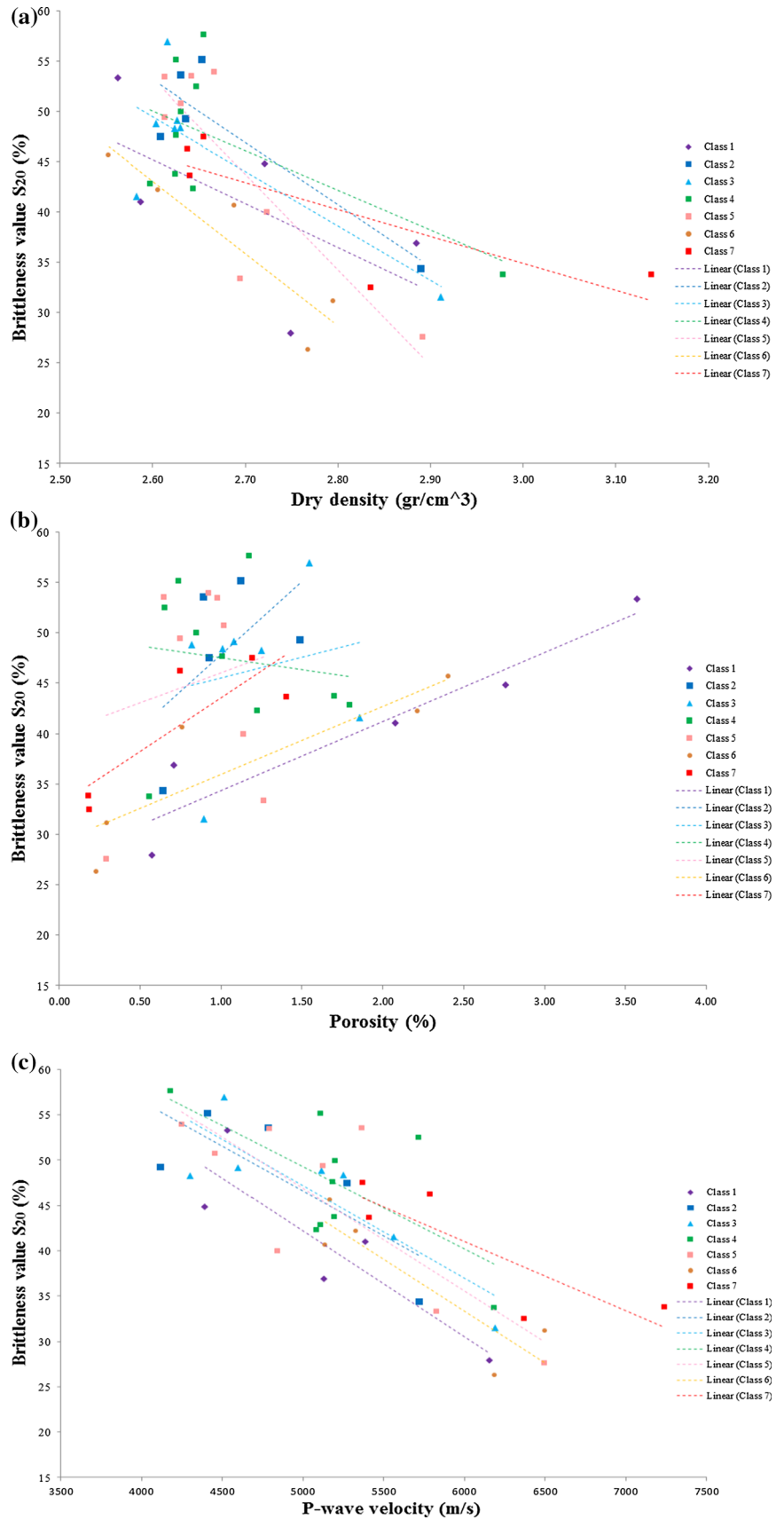
Table 5 Equations between mechanical properties and simple tests for each hardness class

Dependent variable (y)	Hardness class	Independent variable (x)			
		Dry density (g/cm^3)	Porosity (%)	P-wave velocity (m/s)	SH rebound value (R_N)
Point load strength index (MPa)	1	$y = 14.224x - 28.297$	$y = -2.181x + 14.345$	$y = 0.0033x - 6.729$	$y = 0.912x - 32.585$
	2	$y = 10.633x - 19.69$	$y = -3.553x + 12.432$	$y = 0.0022x - 1.715$	$y = -0.575x + 38.25$
	3	$y = 22.677x - 51.84$	$y = -1.204x + 9.852$	$y = 0.0042x - 12.916$	$y = 1.957x - 99.242$
	4	$y = 8.908x - 15.271$	$y = -1.180x + 9.773$	$y = 0.0024x - 4.210$	$y = -0.301x + 25.647$
	5	$y = 9.299x - 16.955$	$y = -3.408x + 10.975$	$y = 0.0017x - 0.559$	$y = -0.992x + 66.993$
	6	$y = 16.802x - 36.809$	$y = -1.455x + 9.962$	$y = 0.0036x - 12.013$	$y = 0.886x - 46.609$
	7	$y = 8.648x - 14.509$	$y = -4.055x + 12.53$	$y = 0.0028x - 7.62$	$y = 1.379x - 78.507$
Brittleness value S_{20} (%)	1	$y = -43.781x + 159.04$	$y = 6.8437x + 27.541$	$y = -0.0117x + 100.57$	$y = -2.625x + 163.65$
	2	$y = -61.986x + 214.31$	$y = 14.597x + 33.241$	$y = -0.0099x + 96.165$	$y = 4.424x - 178.16$
	3	$y = -54.086x + 190.07$	$y = 4.142x + 41.397$	$y = -0.0102x + 98.3$	$y = -5.461x + 346.75$
	4	$y = -39.388x + 152.46$	$y = -2.318x + 49.826$	$y = -0.0091x + 94.598$	$y = -1.322x + 122.55$
	5	$y = -94.851x + 299.87$	$y = 5.918x + 40.135$	$y = -0.0113x + 103.22$	$y = 5.879x - 304.34$
	6	$y = -71.781x + 229.69$	$y = 6.728x + 29.278$	$y = -0.0115x + 102.08$	$y = -5.694x + 389.88$
	7	$y = -26.67x + 114.95$	$y = 10.661x + 32.912$	$y = -0.0076x + 86.869$	$y = -5.938x + 419.98$

Table 6 Results of statistical performance analysis of simple regression models based on hardness classification

Model no.	Dependent variable	Independent variable	RMSE	R	R^2	Adj. R^2	p value
5	Point load strength index (MPa)	Dry density (g/cm^3)	1.42	0.76	0.58	0.57	0.000
6		Porosity (%)	1.59	0.69	0.48	0.47	0.000
7		P-wave velocity (m/s)	1.02	0.89	0.79	0.78	0.000
8		SH rebound value (R_N)	1.69	0.64	0.41	0.40	0.000
5	Brittleness value S_{20} (%)	Dry density (g/cm^3)	4.93	0.83	0.68	0.67	0.000
6		Porosity (%)	6.65	0.65	0.42	0.41	0.000
7		P-wave velocity (m/s)	4.63	0.85	0.72	0.71	0.000
8		SH rebound value (R_N)	6.45	0.68	0.46	0.44	0.000

analysis of the extensive amount of recorded data in the NTNU/SINTEF database of hard rock types. As shown in Fig. 7, model 28 has a good performance for classification of mechanical properties of the studied rocks based on rebound hardness classes, dry density, and P-wave velocity of the samples.

5 Discussion and Classification

According to the results of statistical models, classification of rebound hardness as a dynamic property of the rock materials is a prerequisite task for prediction of mechanical behaviors of igneous rocks and considerably affects the accuracy of the results. In this study, an investigation into the role of rebound hardness on physical, mechanical, and dynamic properties of igneous rocks is presented. For such a purpose, contour diagrams interpolating the contour lines of SH rebound values are used (Figs. 8, 9).

From the results of both simple and multiple linear regression analyses, P-wave velocity was found as an efficient supplementary to the rebound hardness classes for prediction of both point load strength index and brittleness values. In Figs. 8a and 9a, the relationship between above-mentioned properties based on available data in this study (the white stars) is illustrated. Figure 8a shows that there is a systematic relationship between the P-wave velocity, SH rebound value, and point load strength index; in addition, the strength of samples with same P-wave velocity is separated from each other based on their rebound values. For example, the samples with the values of P-wave velocity ranging from 5000 to 5500 m/s have a wide range of point load index between 5.5 and 12.6 MPa, but the strength of the samples can be predicted with a high accuracy by considering the rebound value level curves. However, as expected, some inconsistencies are observed in Figs. 8a and 9a especially in the case of brittleness value—P-wave velocity—SH rebound value contour diagram.

Table 7 Statistic parameters of multiple linear regression between mechanical and simple tests

Model no.	Predictive model	RMSE	R^2	Adj. R^2	p value
9	$I_{s(50)} = 11.079\,\rho - 0.279\,\phi - 20.772$	1.64	0.46	0.43	0.000
10	$I_{s(50)} = 5.913\,\rho + 0.0015\,V_p - 15.333$	1.43	0.59	0.57	0.000
11	$I_{s(50)} = 12.277\,\rho - 0.062\,R_N - 20.783$	1.62	0.48	0.45	0.000
12	$I_{s(50)} = -0.222\,\phi + 0.0021\,V_p - 2.261$	1.53	0.53	0.51	0.000
13	$I_{s(50)} = -1.787\,\phi - 0.130\,R_N + 18.098$	1.92	0.26	0.22	0.002
14	$I_{s(50)} = 0.0027\,V_p - 0.162\,R_N + 3.659$	1.30	0.66	0.64	0.000
15	$I_{s(50)} = 6.019\,\rho + 0.054\,\phi + 0.0016\,V_p - 15.753$	1.45	0.59	0.56	0.000
16	$I_{s(50)} = 10.453\,\rho - 0.674\,\phi - 0.097\,R_N - 13.158$	1.60	0.50	0.46	0.000
17	$I_{s(50)} = 4.514\,\rho + 0.0021\,V_p - 0.147\,R_N - 6.312$	1.25	0.69	0.67	0.000
18	$I_{s(50)} = -0.736\,\phi + 0.0024\,V_p - 0.192\,R_N + 7.659$	1.25	0.70	0.67	0.000
19	$I_{s(50)} = 3.203\,\rho - 0.539\,\phi + 0.0021\,V_p - 0.172\,R_N - 0.486$	1.23	0.71	0.68	0.000
9	$S_{20} = -49.727\,\rho - 0.601\,\phi + 178.65$	6.45	0.47	0.44	0.000
10	$S_{20} = -19.906\,\rho - 0.0072\,V_p + 135.76$	5.19	0.66	0.64	0.000
11	$S_{20} = -47.109\,\rho - 0.140\,R_N + 178.84$	6.42	0.47	0.45	0.000
12	$S_{20} = -1.148\,\phi - 0.0101\,V_p + 98.871$	5.46	0.62	0.60	0.000
13	$S_{20} = 3.963\,\phi - 0.052\,R_N + 42.756$	8.35	0.11	0.07	0.090
14	$S_{20} = -0.0102\,V_p + 0.235\,R_N + 84.738$	5.38	0.63	0.61	0.000
15	$S_{20} = -24.369\,\rho - 2.267\,\phi - 0.0078\,V_p + 153.5$	5.08	0.68	0.65	0.000
16	$S_{20} = -51.12\,\rho - 1.4815\,\phi - 0.216\,R_N + 195.61$	6.45	0.48	0.44	0.000
17	$S_{20} = -18.242\,\rho - 0.0079\,V_p + 0.1745\,R_N + 125.03$	5.18	0.67	0.64	0.000
18	$S_{20} = -0.579\,\phi - 0.0104\,V_p + 0.212\,R_N + 87.886$	5.44	0.63	0.60	0.000
19	$S_{20} = -23.105\,\rho - 2.001\,\phi - 0.0080\,V_p + 0.078\,R_N + 146.65$	5.13	0.68	0.65	0.000

Considering the results shown in Table 8, for a more accurate prediction of both strength and brittleness, a third property is required. The effect of third property is illustrated in Figs. 8b, c and 9b, c. For example, there are two discrepant regions in Fig. 8a: the first region is located between 4200 and 4600 m/s values of P-wave velocity and 5.5–8.5 MPa values of point load index; the other falls between 5700 and 6300 m/s values of P-wave velocity where point load index of the samples is more than 8.5 MPa. As shown in Fig. 8b, in these regions point load strength of the studied rocks can be predicted with a high accuracy, if level curves of dry density will be taken into account. As shown in Figs. 8, 9 and Table 8, among the studied models, dry density, P-wave velocity, and SH rebound value make a fine complement to prediction of both point load strength index and brittleness value.

As presented in Fig. 8, *with same values of P-wave velocity, strength decreases with the increase in SH rebound value.* An explanation for this phenomenon might be the elastic properties of the studied rocks. There are various studies in the literature proposing empirical relationships between strength and both static and dynamic elastic properties of different rock types (Deere and Miller 1966; King 1983; Lashkaripour 2002; Marinos and Tsiambaos 2010; Najibi et al. 2015). Based on the theory of linear elasticity,

the compression modulus or P-wave modulus (M) is one of the elastic moduli available to describe isotropic homogeneous materials. This modulus is defined as the ratio of axial stress to axial strain in a uniaxial strain state:

$$\sigma_{zz} = M\varepsilon_{zz} \tag{5.1}$$

where all the other strains are zero and M is expressed as:

$$M = \rho V_p^2 \tag{5.2}$$

where ρ and V_P are the density and P-wave velocity, respectively. Combining Eqs. (5.1) and (5.2), the P-wave velocity is stated as:

$$V_p = \sqrt{\frac{\sigma_{zz}}{\rho\varepsilon_{zz}}} \tag{5.3}$$

Note that the linear elasticity is a simplification of the more general nonlinear theory of elasticity and is a branch of continuum mechanics. In linear elasticity, the fundamental assumptions are small deformations (or strains) and linear relationships between the components of stress and strain, which are valid only for stress states that do not produce yielding. In practice, linear elasticity theory is applicable to a wide range of natural and engineering materials and thus extensively used in structural analysis and engineering design (Wang et al. 2015).

Table 8 Results of statistical performance analysis of multiple regression models based on hardness classification

Model no.	Dependent variable	Independent variables	RMSE	R^2	Adj. R^2	p value
20	Point load strength index	Dry density − porosity	1.33	0.646	0.63	0.000
21		Dry density − P-wave velocity	0.94	**0.821**	0.81	0.000
22		Dry density − SH rebound value	1.30	0.662	0.65	0.000
23		Porosity − P-wave velocity	0.98	0.806	0.80	0.000
24		Porosity − SH rebound value	1.52	0.539	0.52	0.000
25		P-wave − SH rebound value	0.96	0.815	0.81	0.000
26		Dry density − porosity − P-wave velocity	0.94	**0.827**	0.81	0.000
27		Dry density − porosity − SH rebound value	1.28	0.678	0.65	0.000
28		Dry density − P-wave velocity − SH rebound value	0.91	**0.838**	0.83	0.000
29		Porosity − P-wave velocity − SH rebound value	0.96	0.820	0.81	0.000
30		Dry density − porosity − P-wave velocity − SH rebound value	0.92	**0.839**	0.82	0.000
20	Brittleness value S_{20}	Dry density − porosity	4.89	0.690	0.68	0.000
21		Dry density − P-wave velocity	3.98	**0.798**	0.79	0.000
22		Dry density − SH rebound value	4.80	0.706	0.69	0.000
23		Porosity − P-wave velocity	4.63	0.726	0.71	0.000
24		Porosity − SH rebound value	6.25	0.502	0.48	0.000
25		P-wave velocity − SH rebound value	4.49	0.743	0.73	0.000
26		Dry density − porosity − P-Wave velocity	4.02	**0.799**	0.78	0.000
27		Dry density − porosity − SH rebound value	4.85	0.708	0.69	0.000
28		Dry density − P-wave velocity − SH rebound value	3.99	**0.801**	0.79	0.000
29		Porosity − P-Wave velocity − SH rebound value	4.54	0.743	0.72	0.000
30		Dry density − porosity − P-wave velocity − SH rebound value	4.02	**0.803**	0.78	0.000

Bold values indicate the strongest relation
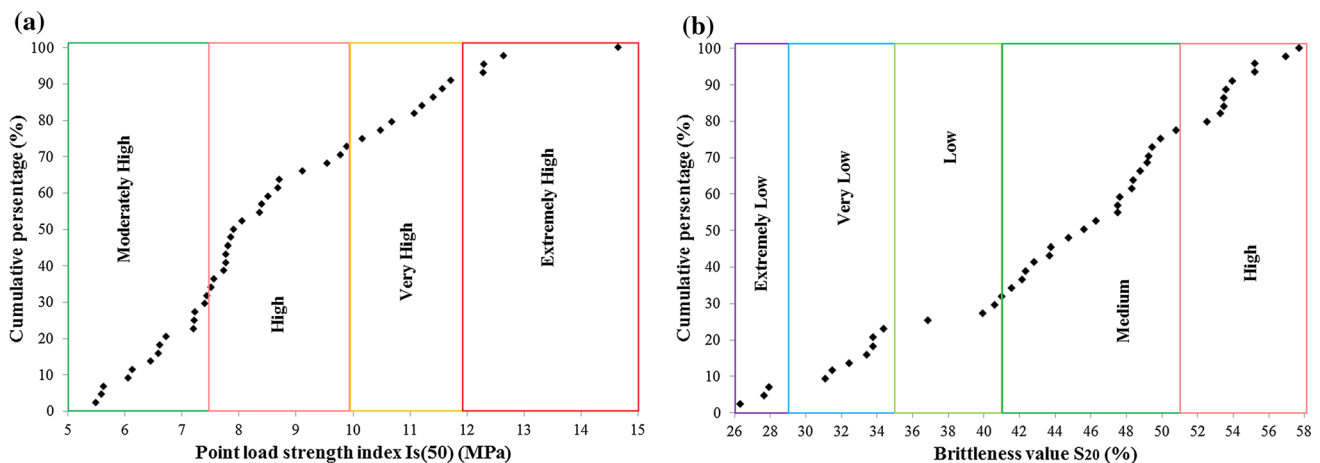
Fig. 6 Classification ranges and statistical distribution of the point load strength index $I_{s(50)}$ values (**a**) and the brittleness values (S_{20}) (**b**) of the studied rocks

Hardness is a complex property and dependent on ductility, elasticity, plasticity, strain, strength, toughness, viscoelasticity, and viscosity (Martin 2011). The hardness of a material is usually defined as its resistance to local plastic deformations (Ohring 1992). In many cases, hardness is defined by the type of test used to measure it. Hardness is characterized in various forms, including scratch hardness, indentation hardness, and rebound hardness. Rebound hardness, also known as dynamic hardness, is related to elasticity (Martin 2011). Defining hardness, H, as the resistance to deformation (strain), there is an inverse ratio between hardness and strain:

$$H \propto \frac{1}{\varepsilon} \tag{5.4}$$
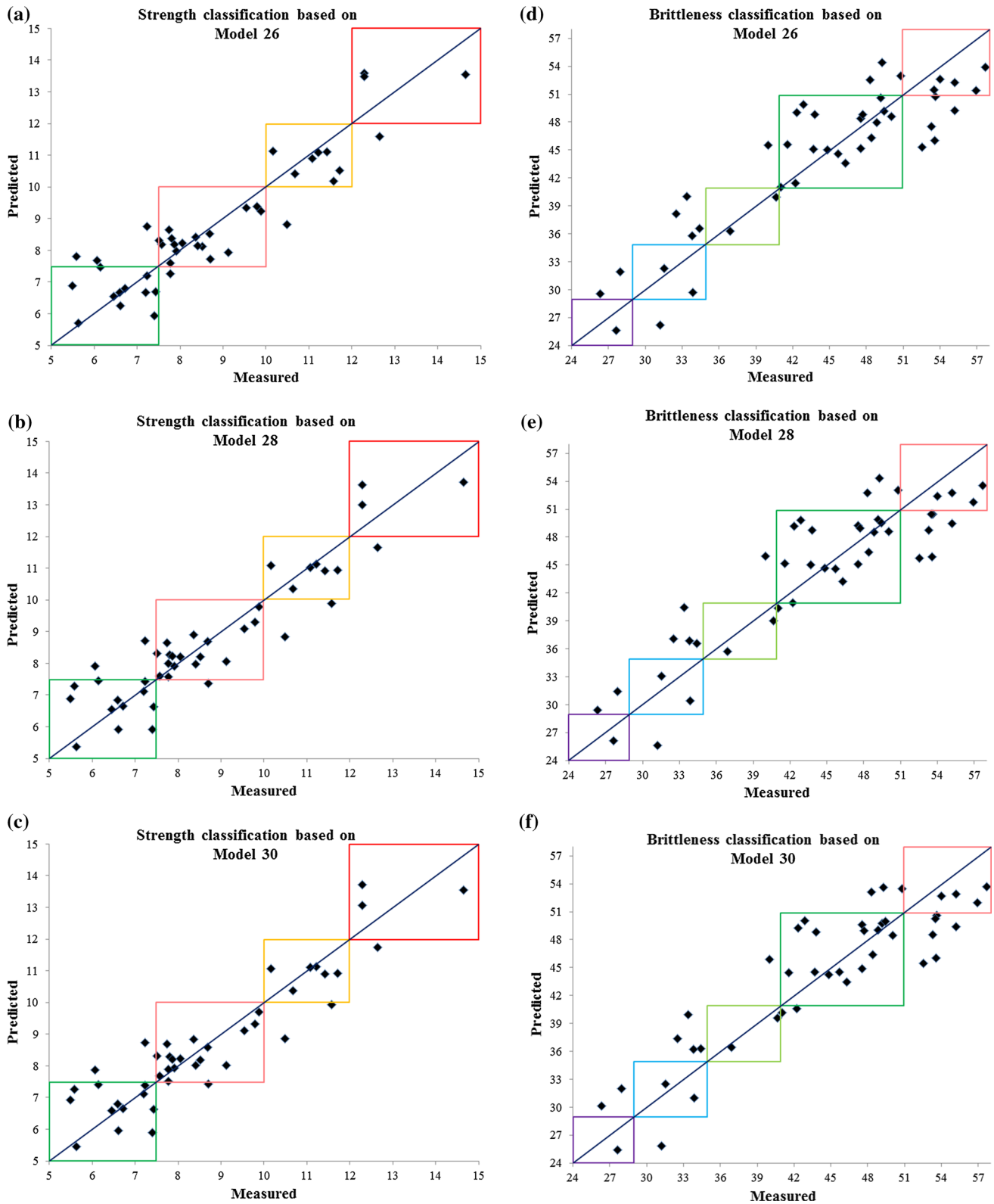
Fig. 7 Graphs of the predicted $I_{s(50)}$ versus the measured $I_{s(50)}$ for the best predictive models of point load strength index, the colored borders refer to $I_{s(50)}$ classification ranges given by the study (**a–c**), and the predicted S_{20} versus measured S_{20} graphs for the best brittleness value predictive models, the colored borders refer to S_{20} classification ranges given by Dahl et al. (2012) (**d–f**)

Fig. 8 Point load strength index $I_{s(50)}$ versus P-wave velocity contour maps: interpolated contour lines of SH rebound values (**a**), SH rebound and dry density values (**b**) and SH rebound and porosity values (**c**) of the studied rocks (*white stars*)
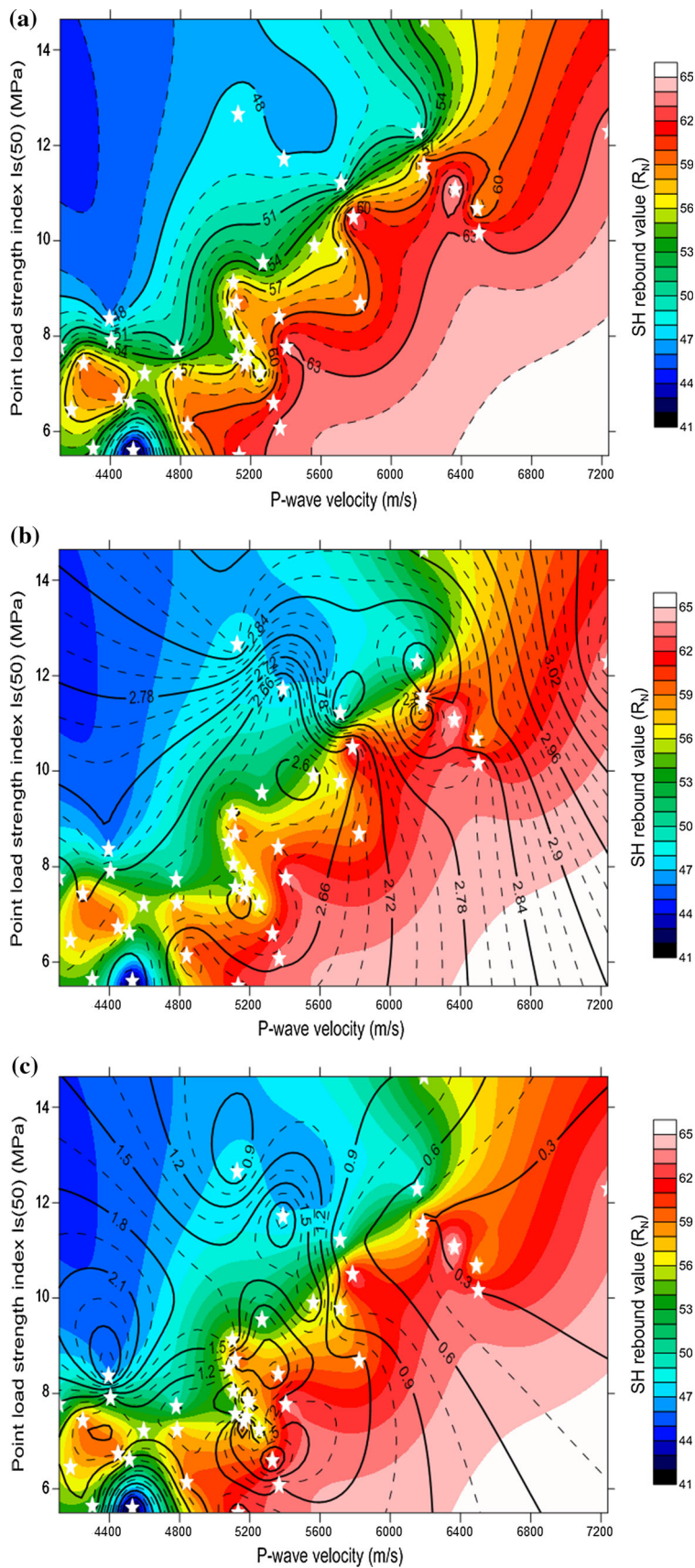
Fig. 9 Brittleness value S(20) versus P-wave velocity contour maps: interpolated contour lines of SH rebound values (**a**), SH rebound and dry density values (**b**) and SH rebound and porosity values (**c**) of the studied rocks (*white stars*)
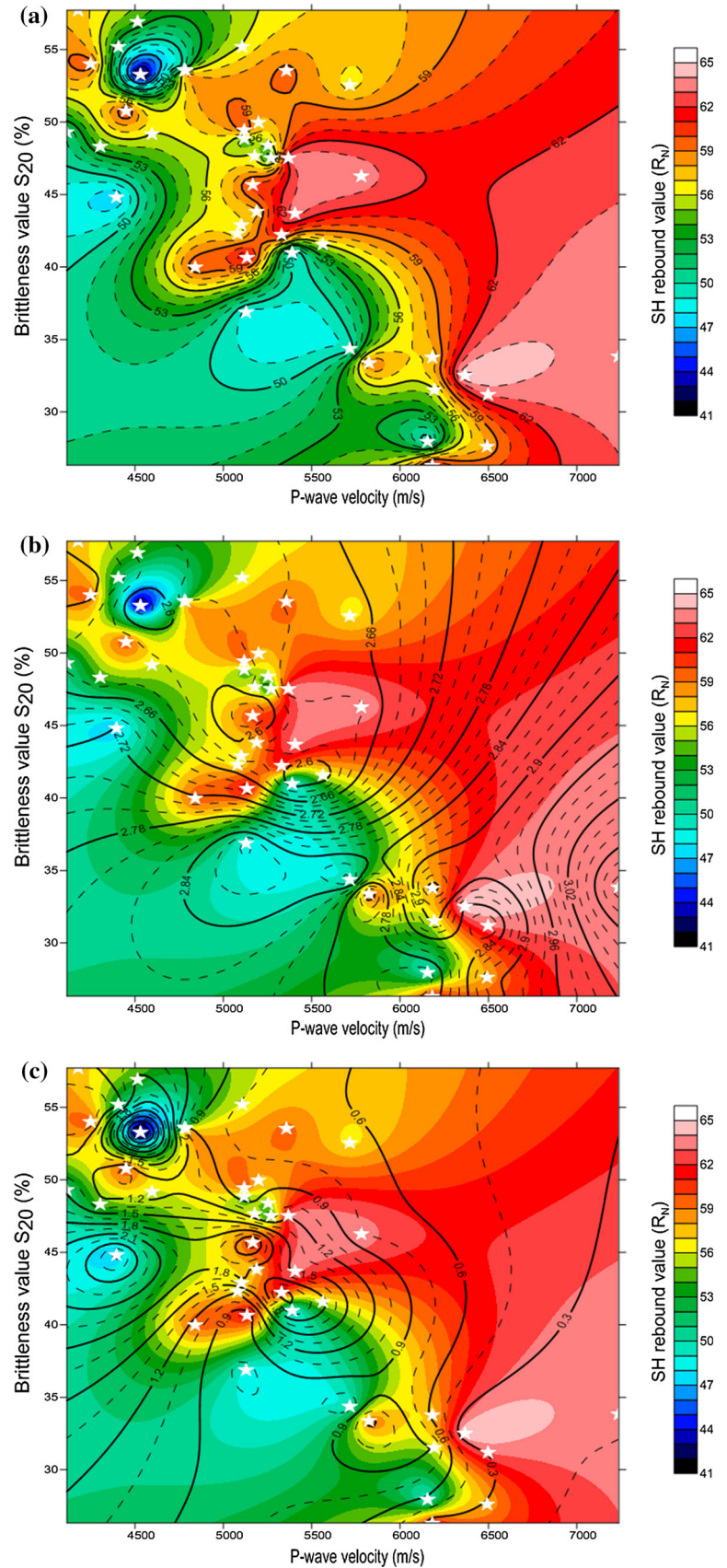
Consequently, if V_P remains unchanged, from Eq. (5.3) at identical values of density, stress has an inverse relationship with hardness. Brady and Brown (2004) defined the strength of rock as follows: "Strength, or peak strength, is the maximum stress, usually averaged over a plane that the rock can sustain under a given set of conditions." Based on this definition, the presented concepts and equations in this section, and the experimental report from the study, with same values of P-wave velocity and dry density, strength (maximum stress that the rock can sustain) decreases with the increase in rebound hardness.

It is worth mentioning that here the deformation of isotropic homogeneous materials is taken into account. Rocks usually are not homogeneous and made up of multiple components such as mineral grains and pore space. Deformation of a single-phase polycrystalline material (such as mineral and rock) can be treated in a similar way: each single crystal with a different orientation can be considered as a material with different mechanical properties (Karato 2008). For such materials, effective modulus often called the Hill average (1952) is used. There is no theoretical reason to justify this model, but it has been frequently used for practical applications (Karato 2008). The Voigt–Reuss–Hill average is used to estimate the effective elastic moduli of a rock in terms of its constituents and pore space (Mavko et al. 2009) as follows:

$$M_{VRH} = \frac{M_V + M_R}{2} \tag{5.5}$$

where Voigt–Reuss–Hill average (M_{VRH}) is simply the arithmetic average of the isostrain or Voigt upper bound effective elastic modulus (M_V);

$$M_V = \sum_{i=1}^{N} f_i M_i \tag{5.6}$$

and the isostress or Reuss lower bound effective elastic modulus (M_R):

$$\frac{1}{M_R} = \sum_{i=1}^{N} \frac{f_i}{M_i} \tag{5.7}$$

the terms f_i and M_i are, respectively, the volume fraction and the modulus of the ith component of a mixture of N material phases (minerals or crystals and pores in rock materials). It is notable that M_{VRH} decreases linearly with porosity. Several authors have shown that the average of these bounds can be a useful and sometimes accurate estimate of rock properties (Mavko et al. 2009).

According to Eqs. (5.2), (5.5)–(5.7), if the effect of Poisson's ratio is neglected and rock is considered as an isotropic material, based on the theory of linear elasticity, the effective P-wave modulus of a rock (M_{Rk}) can be written as follows:

$$M_{Rk} = \left[\left(\sum_{i=1}^{N} f_i \rho_i \left(V_p^2 \right)_i \right) + \left(1 / \sum_{i=1}^{N} \frac{f_i}{\rho_i \left(V_p^2 \right)_i} \right) \right] / 2 \tag{5.8}$$

Finally, combining Eqs. (5.1), (5.4), and (5.8) gives:

$$(\sigma_{max})_{zz} \propto \frac{\left[\left(\sum_{i=1}^{N} f_i \rho_i \left(V_p^2 \right)_i \right) + \left(1 / \sum_{i=1}^{N} \frac{f_i}{\rho_i \left(V_p^2 \right)_i} \right) \right]}{2 \left(\sum_{i=1}^{N} f_i H_i \right)} \tag{5.9}$$

Therefore, in rock materials, the relationships among strength, hardness, density, and P-wave velocity can exist in each constituent. It is recalled that hardness is defined as the resistance to plastic deformation, and at peak rock strength point (maximum stress), rocks mainly have plastic behavior.

It can be derived from Eq. (5.9) that mineral composition and density are two key properties controlling the mechanical and dynamic properties of rock materials. According to Birch's law (1961), seismic wave velocities are the linear functions of density and the effect of a chemical composition mainly through the mean atomic weight. Thus, when P-wave velocity and density are considered, the mineral chemical composition would be taken into account. From the theoretical concepts and experimental studies, it might be concluded that density, P-wave velocity, and rebound hardness make a fine complement to mechanical properties classification of rock materials.

It has long been known that point load strength results can be used for rock strength classification (Broch and Franklin 1972; Bieniawski 1984, 1989; Ghosh and Srivastava 1991). From the results of this study, including laboratory tests (Table 2) and experimental observations, regression analysis (Tables 3, 6, 7, 8), classification accuracy between measured and predicted values from the best models (Fig. 7), contour diagrams (Fig. 8), and theoretical concepts, a chart was prepared for strength classification of igneous rocks (Fig. 10). Dry density, P-wave velocity, and Schmidt rebound number of the samples are used as input parameters in the proposed chart to classify the strength of the rock. As presented in Fig. 10a, there are several dry density–P-wave velocity (DP) boxes in the chart, which are constructed from 3 categories of dry density and three categories of P-wave velocity. In order to strength classification using the chart, first of all, the related DP box of the sample must be specified, and then, strength class of intact rock is determined by corresponding hardness class (Table 4) in selected DP box. As shown in Fig. 10b, only four samples, marked by bold borders, were misclassified according to the proposed chart. Notice that the point load strength index of three mentioned results, i.e., (R5), (R8$_{(b)}$), and (R9$_{(a)}$) samples, is equal to 7.77, 7.23, and 9.54, respectively, indicating small errors, and the other one (R25) is an
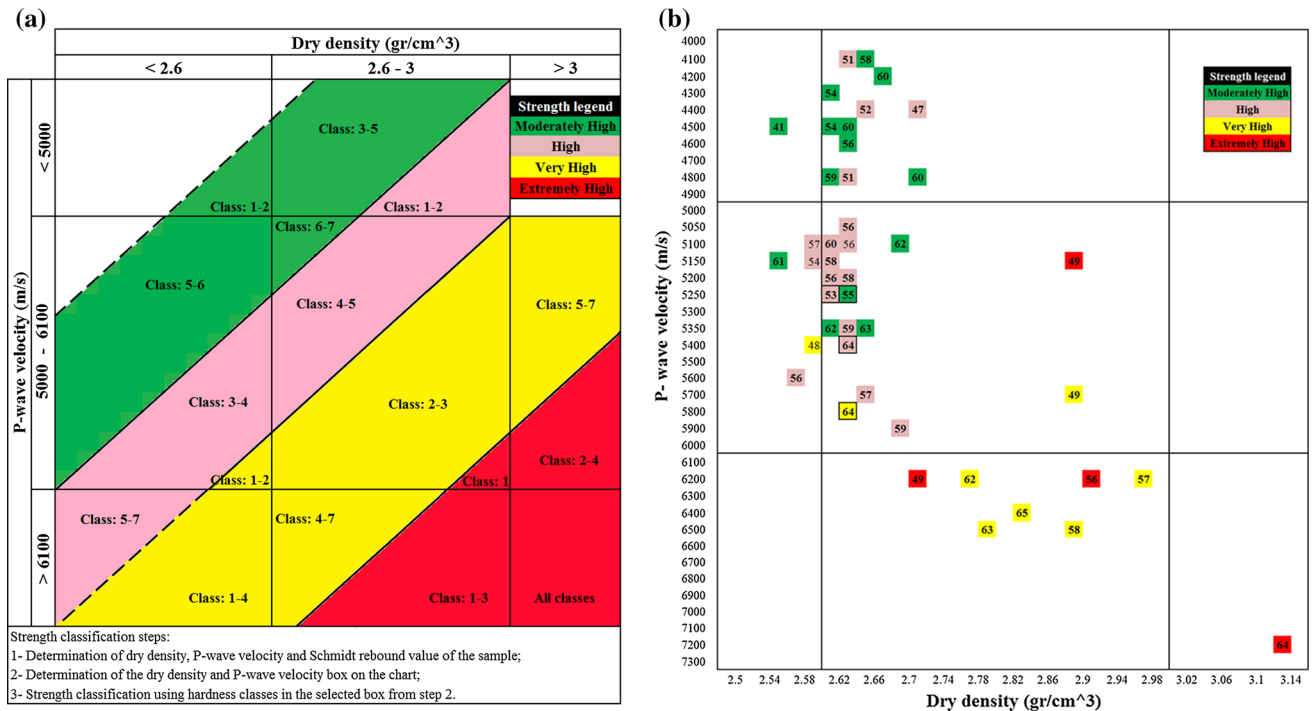
Fig. 10 **a** Strength classification chart of igneous rocks using simple methods and **b** P-wave velocity versus dry density of the studied rocks for different strength classes (*color* of the plotted samples) and SH rebound values (*numbers* inside the plotted samples) (color figure online)
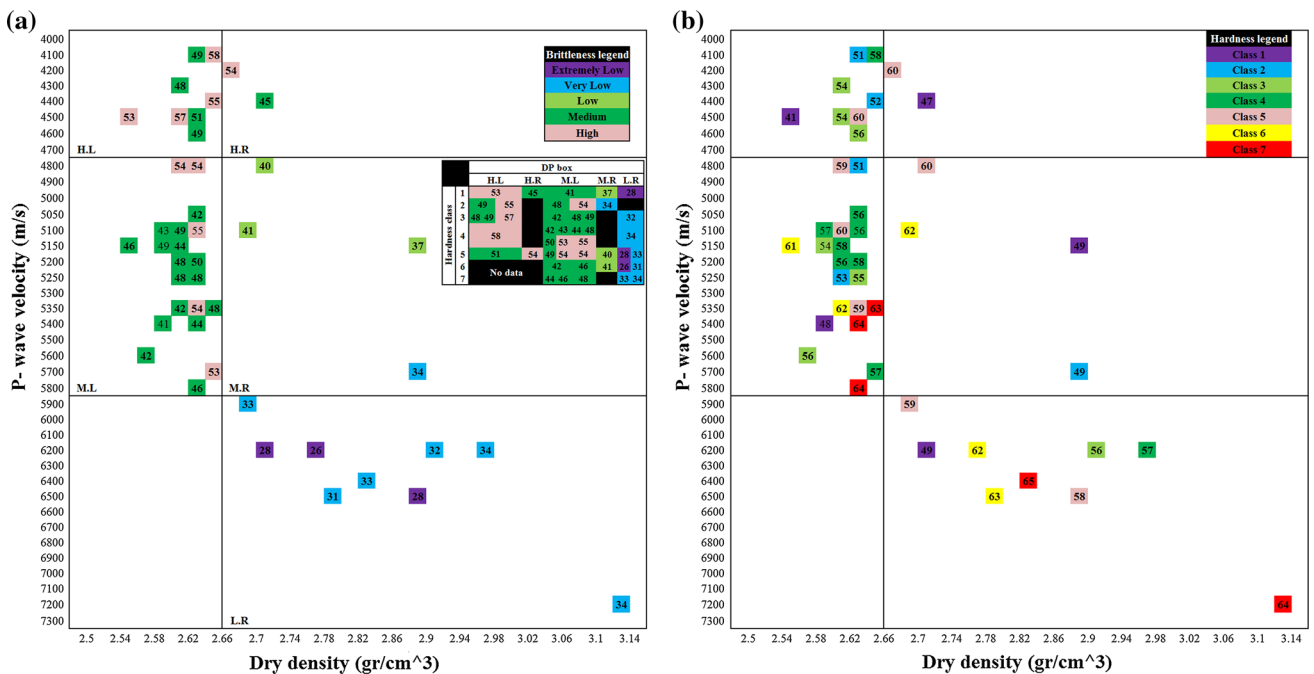
Fig. 11 **a** P-wave velocity versus dry density of the studied rocks for different brittleness classes (*color* of the plotted samples) and S_{20} values (*numbers* inside the plotted samples) and **b** P-wave velocity versus dry density of the studied rocks for different hardness classes (*color* of the plotted samples) and SH rebound values (*numbers* inside the plotted samples) (color figure online)

extrusive rock. This inconsistency shows that more consideration is required to deal with extrusive rocks, which have more structural complexity.

About the rock brittleness, as shown in Fig. 11, rocks with different hardness classes behave differently probably because of the elastic properties of the studied rocks. There

Table 9 Brittleness value S_{20} classification of the studied rocks

Dry density (g/cm^3)	P-wave velocity (m/s)	S_{20} (%)	Brittleness category (Dahl et al. 2012)
<2.66	<4800	47–59	Medium–high
	4800–5900	41–56	Medium–high
	>5900	34–47	Very low–medium
>2.66	<4800	41–56	Medium–high
	4800–5900	34–47	Very low–medium
	>5900	25–34	Extremely low–very low

is a systematic trend between brittleness and corresponding hardness classes of the samples in different DP boxes (Fig. 11). For instance, as shown in the inset table of Fig. 11a, in each DP box, samples classified into medium hardness classes (3–5) have higher brittleness values. However, presentation a quantitative classification chart with respect to hardness needs more data from different rock types. Based on the dataset prepared in this study, a table for brittleness value S_{20} classification of igneous rocks based on P-wave velocity and dry density was presented (Table 9). The rebound hardness, as a qualitative parameter, can be used considering the inset table of Fig. 11a. However, as mentioned by some authors, brittleness is a complex property and is dependent on various rock properties. It seems that one of the most important properties affecting the brittleness of rocks is petrographic characteristics such as grain size and texture features. Therefore, for a more detailed classification of brittleness, such characteristics must be taken into account. As shown in Figs. 10 and 11, an igneous rock can be both brittle and strong, but generally stronger rocks show a lower brittleness.

6 Conclusions

Based on experimental observations, statistical models, and theoretical concepts, we proposed a novel engineering classification of the strength and brittleness of igneous rocks. The proposed classification is based on the integration of three simple parameters including dry density, P-wave velocity, and SH rebound value and is designed to allow a rapid assessment of the engineering properties of igneous rocks. The proposed methods provide reliable and inexpensive procedures for strength and brittleness classification of igneous rocks. The classification could (in many cases) help avoid time-consuming and tedious test methods. Furthermore, subsequent research could efficiently integrate the presented strength classification chart with rock mass classification systems for the task of rock mass classification. Overall, based on the results of this study, the following conclusions may be reached:

1. The results from statistical models demonstrate that rocks with different hardness values have different physicomechanical properties or relations. In addition, classification of rebound hardness as a dynamic property of the rock materials is a prerequisite task for prediction of mechanical behaviors of igneous rocks.

2. Based on the results from statistical models and theoretical concepts, we conclude that dry density, P-wave velocity, and SH rebound value provide a fine complement to mechanical properties classification of rock materials. Notably, such properties incorporate the effect of elastic properties and mineral composition of rock materials.

3. With limited ranges of P-wave velocity and dry density, strength decreases with an increase in SH rebound value.

4. There is a systematic trend between dry density, P-wave velocity, rebound hardness, and brittleness value of the studied rock, and rocks with medium hardness have higher brittleness values.

Further research is necessary to check the validity of the presented classifications for other rock types. In addition, the effect of petrographic features on the developed classifications must be investigated. Finally, it is recommended to classify other rock strength parameters such as UCS and Brazilian tensile strength using the presented strength classification chart.

References

Altindag R (2010) Assessment of some brittleness indexes in rock drilling efficiency. Rock Mech Rock Eng 43:361–370

Andreev GE (1995) Brittle failure of rock materials: test results and constitutive models. Balkema/Rotterdam, A. A, p 446

Anon (1995) The description and classification of weathered rocks for engineering purposes. Geological Society Engineering Group Working Party Report. Q J Eng Geol 28:207–242

Aydin A (2009) ISRM suggested method for determination of the Schmidt hammer rebound hardness: revised version. Int J Rock Mech Min Sci 46:627–634

Beiki M, Majdi A, Givshad AD (2013) Application of genetic programming to predict the uniaxial compressive strength and

elastic modulus of carbonate rocks. Int J Rock Mech Min Sci 63:159–169

Bieniawski ZT (1984) Rock mechanics design in mining and tunneling. A.A Balkema, Rotterdam, p 272

Bieniawski ZT (1989) Engineering rock mass classifications. Wiley, New York, p 251

Birch F (1961) The velocity of compressional waves in rocks to 10 kilobars, Part 2. J Geophys Res 66:2199–2224

Blindheim OT, Bruland A (1998) Boreability testing, in Norwegian TBM Tunnelling, Publication No. 11, Norwegian Tunnelling Society

Brady BHG, Brown ET (2004) Rock mechanics for underground mining. George Allen & Unwin, London, p 628

Broch EM, Franklin JA (1972) The point load strength test. Int J Rock Mech Min Sci Geomech Abstr 9:669–697

Copur H, Bilgin N, Tuncdemir H, Balci C (2003) A set of indices based on indentation test for assessment of rock cutting performance and rock properties. J S Afr Inst Min Metall 103(9):589–600

Dahl F (2003) DRI, BWI, CLI standards. NTNU, Angleggsdrift, Trondheim, p 20

Dahl F, Bruland A, Jakobsen PD, Nilsen B, Grov E (2012) Classifications of properties influencing the drillability of rocks, based on the NTNU/SINTEF test method. Tunn Undergr Space Technol 28:150–158

Davis JC (1973) Statistics and data analysis in geology. Wiley, New York, p 550

Deere DU, Miller RP (1966) Engineering classification and index properties for intact rocks. Tech Rep no. AFNL-TR-65-116, Air Force Weapons Laboratory, New Mexico, p 300

Dursun AE, Gokay MK (2016) Cuttability assessment of selected rocks through different brittleness values. Rock Mech Rock Eng 49(4):1173–1190

Ghosh DK, Srivastava M (1991) Point-load strength: an index for classification of rock material. Bull Int Assoc Eng Geol 44:27–33

Gong QM, Zhao J (2007) Influence of rock brittleness on TBM penetration rate in Singapore granite. Tunn Undergr Space Technol 22:317–324

Gupta V, Sharma R (2012) Relationship between textural, petrophysical and mechanical properties of quartzites: a case study from northwestern Himalaya. Eng Geol 135–136:1–9

Gurocak Z, Solanki P, Alemdag S, Zaman MM (2012) New considerations for empirical estimation of tensile strength of rocks. Eng Geol 145–146:1–8

Hajiabdolmajid V, Kaiser P (2003) Brittleness of rock and stability assessment in hard rock tunnelling. Tunn Undergr Space Technol 18:35–48

Hawkins AB (1998) Aspects of rock strength. Bull Eng Geol Environ 57:17–30

Heidari M, Khanlari G, Torabi-Kaveh M, Kargarian S (2012) Predicting the uniaxial compressive and tensile strengths of gypsum rock by point load testing. Rock Mech Rock Eng 45(2):265–273

Hill R (1952) The elastic behaviour of a crystalline aggregate. Proc Phys Soc Lond A 65:349–354

Hunka V, Das B (1974) Brittleness determination of rocks by different methods. Int J Rock Mech Min Sci Geomech Abst 11:389–392

Inoue M, Ohomi M (1981) Relation between uniaxial compressive strength and elastic wave velocity of soft rock. In: Proceedings of the international symposium on weak rock, Tokyo, pp 9–13

ISRM (1981) Rock characterization, testing and monitoring, ISRM suggested methods. Pergamon, Oxford, p 211

ISRM (1985) Suggested methods for determining point load strength. Int J Rock Mech Min Sci Geomech Abstr 22(2):51–60

ISRM (2007) The Complete ISRM Suggested Methods for Rock Characterization, Testing and Monitoring: 1974–2006. In: R Ulusay, JA Hudson (eds.), Suggested methods prepared by the commission on testing methods, International Society for Rock Mechanics, Compilation Arranged by the ISRM Turkish National Group, Ankara, P 293

Kahraman S (2001) Evaluation of simple method for assessing the uniaxial compressive strength of rock. Int J Rock Mech Min Sci 38:981–994

Kahraman S, Bilgin N, Feridunoglu C (2003) Dominant rock properties affecting the penetration rate of percussive drills. Int J Rock Mech Min Sci 40:711–723

Karakus M, Tutmez B (2006) Fuzzy and multiple regression modelling for evaluation of intact rock strength based on point load, Schmidt hammer and sonic velocity. Rock Mech Rock Eng 39(1):45–57

Karato SI (2008) Deformation of earth materials. New York, Cambridge University Press, p 463

Katz O, Reches Z, Roegiers JC (2000) Evaluation of mechanical rock properties using a Schmidt Hammer. Int J Rock Mech Min Sci 37:723–728

Khandelwal M, Ranjith PG (2010) Correlating index properties of rocks with P-wave measurements. J Appl Geophys 71:1–5

Kilic A, Teymen A (2008) Determination of mechanical properties of rocks using simple methods. Bull Eng Geol Environ 67(2):237–244

King MS (1983) Static and dynamic elastic properties of rock from the Canadian Shield. Int J Rock Mech Min Sci Geomech Abstr 20(5):237–241

Kohno M, Maeda H (2012) Relationship between point load strength index and uniaxial compressive strength of hydrothermally altered soft rocks. Int J Rock Mech Min Sci 50:147–157

Lashkaripour GR (2002) Predicting mechanical properties of mudrock from index parameters. Bull Eng Geol Environ 61(1):73–77

Lawn BR, Marshall DB (1979) Hardness, toughness and brittleness: an indentation analysis. J Ceram Soc 62(78):347–350

Li D, Wong LNY (2013) Point load test on meta-sedimentary rocks and correlation to UCS and BTS. Rock Mech Rock Eng 46:889–896

Liu Z, Shao J, Xu W, Wu Q (2014) Indirect estimation of unconfined compressive strength of carbonate rocks using extreme learning machine. Acta Geotech. doi:10.1007/s11440-014-0316-1

Marinos PV, Tsiambaos G (2010) Strength and deformability of specific sedimentary and ophiolitic rocks. In: Proceedings of the 12th international congress, Patras, bulletin of the geological society of Greece, XLIII, vol 3, pp 1259–1266

Martin PM (2011) Introduction to surface engineering and functionally engineered materials. Wiley, New York, p 565

Mavko G, Mukerji T, Dvorkin J (2009) The rock physics handbook: tools for seismic analysis of porous media. Cambridge University Press, Cambridge, p 511

Minaeian B, Ahangari K (2013) Estimation of uniaxial compressive strength based on P-wave and Schmidt hammer rebound using statistical method. Arab J Geosci 6:1925–1931

Monjezi M, Khoshalan HA, Razifard M (2012) A neurogenetic network for predicting uniaxial compressive strength of rocks. Geotech Geol Eng 30:1053–1062

Najibi AR, Ghafoori M, Lashkaripour GR, Asef MR (2015) Empirical relations between strength and static and dynamic elastic properties of Asmari and Sarvak limestones, two main oil reservoirs in Iran. J Pet Sci Eng 126:78–82

Obert L, Duvall WI (1967) Rock mechanics and the design of structures in rock. Wiley, New York, p 278

Ohring M (1992) The materials science of thin films. Academic Press, New York, p 704

Palchik V, Hatzor YH (2004) The influence of porosity on tensile and compressive strength of porous chalks. Rock Mech Rock Eng 37(4):331–341

Protodyakonov MM (1963) Mechanical properties and drillability of rocks. In: Proceedings of the 5th symposium rock mechanics, University of Minnesota, pp 103–118

Quinn JB, Quinn GD (1997) Indentation brittleness of ceramics: a fresh approach. J Mater Sci 32:4331–4346

Rabbani E, Sharif F, KoolivandSalooki M, Moradzadeh A (2012) Application of neural network technique for prediction of uniaxial compressive strength using reservoir formation properties. Int J Rock Mech Min Sci 56:100–111

Ramsey JG (1967) Folding and fracturing of rocks. McGraw-Hill, London, p 289

Reichmuth DR (1968) Point-load testing of brittle materials to determine tensile strength and relative brittleness. In: Proceedings of 9th symposium on rock mech, pp 134–159

Rezaei M, Majdi A, Monjezi M (2012) An intelligent approach to predict unconfined compressive strength of rock surrounding access tunnels in longwall coal mining. Neural Comput Appl 24:233–241

Sharma PK, Singh TN (2008) A correlation between P-wave velocity, impact strength index, slake durability index and uniaxial compressive strength. Bull Eng Geol Environ 67:17–22

Shorey PR, Barat D, Das MN, Mukherjee KP, Singh B (1984) Schmidt hammer rebound data for estimation of large scale in situ coal strength. Int J Rock Mech Min Sci Geomech Abst 21:39–42

Singh SP (1986) Brittleness and the mechanical winning of coal. Min Sci Technol 3:173–180

Streckeisen A (1976) To each plutonic rock its proper name. Earth Sci Rev 12:12–33

von Matern N, Hjelmer A (1943) Forsok med pagrus (''Tests with Chippings''), Medelande nr. 65, Statens vaginstitut, Stockholm (English summary, pp 56–60)

Wang B, Xia K, Wei GW (2015) Matched interface and boundary method for elasticity interface problems. J Comput Appl Math 285:203–225

Yagiz S (2002) Development of rock fracture and brittleness indices to quantify the effects of rock mass features and toughness in the CSM Model basic penetration for hard rock tunneling machines, Ph.D. thesis, Colorado School of Mines, USA

Yagiz S (2009a) Assessment of brittleness using rock strength and density with punch penetration test. Tunn Undergr Space Technol 24:66–74

Yagiz S (2009b) Predicting uniaxial compressive strength, modules of elasticity and index properties of rocks using the Schmidt hammer. Bull Eng Geol Environ 68:55–63

Yagiz S, Sezer EA, Gokceoglu C (2012) Artificial neural networks and nonlinear regression techniques to assess the influence of slake durability cycles on the prediction of uniaxial compressive strength and modulus of elasticity for carbonate rocks. Int J Numer Anal Meth Geomech 36:1636–1650

Yarali O, Kahraman S (2011) The drillability assessment of rocks using the different brittleness values. Tunn Undergr Space Technol 26:406–414